Adsorption of Carbon Dioxide in Non-Löwenstein Zeolites

CHEMISTRY OF MATERIALS

pubs.acs.org/cm

Article

Adsorption of Carbon Dioxide in Non-Löwenstein Zeolites

Pablo Romero-Marimon, Juan José Gutiérrez-Sevillano,* and Sofia Calero*

Cite This: *Chem. Mater.* 2023, 35, 5222−5231

Read Online

ACCESS | Metrics & More | Article Recommendations | Supporting Information

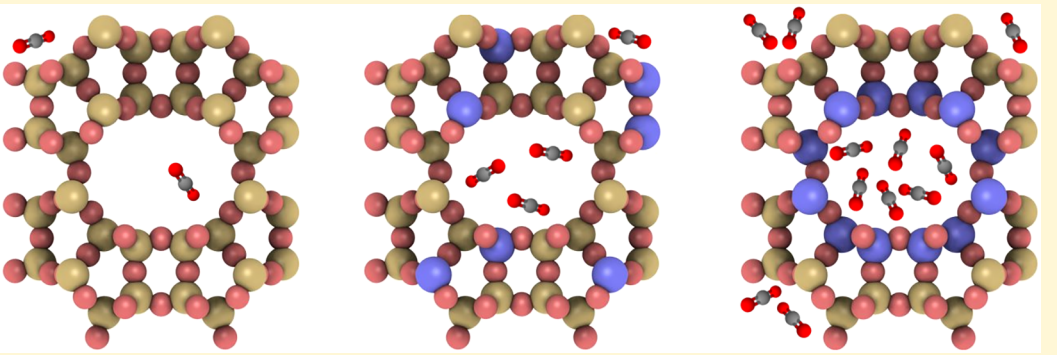

ABSTRACT: We investigated the effect of the aluminum distribution in the adsorption properties of carbon dioxide in the MFI, MOR, and ITW zeolites. Because of its lack of experimental evidence and theoretical validation, Löwenstein's rule was not generally imposed, and special attention was paid to the effect of the Al−O−Al linkages. To this end, we first generalized an existing transferable force field for CO_2 adsorption in non-Löwenstein zeolites. By means of molecular simulations based on this force field, we showed that the carbon dioxide adsorption efficiency in MFI is determined by the number of Al atoms, rather than by their distribution in the framework. This was attributed to the small size of the CO_2 molecules compared to the 3D wide-channel topology of the structure. Conversely, we found that the Al distribution has a higher impact on the heat of adsorption in MOR. Although structures with a very high and very low number of non-Löwenstein bonds presented significant differences, the bonds themselves do not affect the heat of adsorption directly. Instead, we found that an homogeneous distribution of the Al atoms in the sites forming the C-channel is more favorable. Finally, the small-pore distribution of the ITW zeolite led to high values of the heat of adsorption and wide error bars, which made the study feasible just for low aluminum concentrations. In that case, we report a small dependency of the heat of adsorption on the Al distribution.

INTRODUCTION

Over the past years, the use of nanoporous materials to adsorb and separate carbon dioxide has gained interest as a potential method for carbon capture.[1] Although a variety of porous solids have received much attention in the past decades, zeolites are the most widely used in industry.[2,3] This is due to their low cost,[4] availability, high thermal stability,[5] and high number of synthesizable topologies with different pore distributions.[6] Even though many new adsorbents like metal−organic frameworks are emerging as an alternative as they display excellent gas adsorption performances,[3,7,8] the use of these frameworks is still very restricted by their high production cost, poor selectivity, and difficulties in regeneration.[9]

The adsorption performance of zeolites depends on the operating conditions. The temperature, pressure, and moisture content seem to be the most relevant factors in the adsorption of carbon dioxide.[10] As expected in most solid−gas systems, a higher efficiency of adsorption is in general achieved for high gas pressures and low temperatures. However, the adsorption efficiency is also strongly dependent on the structural properties of the zeolite. In fact, different topologies might perform differently with different adsorbates, depending on their size and polarity. Besides, for a given topology, multiple Si/Al ratios and distributions of the aluminum atoms can also lead to different results.[11−13] The substitution of Si atoms with Al atoms leads to a negative net charge in the framework, which needs to be compensated by introducing extraframework cations. Because the cation distribution is highly dependent on the positions of the aluminum substitutions, these have an impact on the number and position of Bronsted acid sites, which determine the interactions between the zeolite and the adsorbates. In particular, the cations increase the interactions between the framework and the CO_2 molecules,

Received: May 23, 2023
Revised: June 10, 2023
Published: June 27, 2023

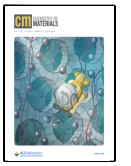

https://doi.org/10.1021/acs.chemmater.3c01258
Chem. Mater. 2023, 35, 5222−5231

favoring adsorption, but they also reduce the adsorption capacity. Therefore, there is a balance between the strength of the framework−adsorbate interactions and the availability of space. It is not clear which Si/Al ratio leads to a better performance and which is the optimal distribution of the Al atoms.

In this context, the so-called Löwenstein's rule,[14] introduced for the first time in 1954, has been generally accepted. This rule prohibits the bonding between two Al atoms through a single oxygen (Al−O−Al) and has been traditionally supported by many experimental studies. Nevertheless, a solid theory on the instability of the Al−O−Al linkage is still missing, and many recent studies have found violations of this rule.[15−18] Moreover, theoretical studies concluded that although it seems to be a small energetic preference for the Löwenstein model, this would be sufficiently small to be overcome by thermal fluctuations even at room temperature.[19] This barrier should be understood as the energetic preference to form Löwenstein over non-Löwenstein structures when zeolites are prepared by normal hydrothermal routes. Overall, as the presence of non-Löwenstein bonds could potentially improve some properties of zeolites,[15] the aforementioned works have opened a new research line in the study of these materials.

In this work, we aimed to study the influence of different aluminum distributions in zeolites in the adsorption of CO_2. Even though the role of aluminum short-range ordering has been studied in the Löwenstein case,[20] many questions remain unknown. To this end, we used Monte Carlo simulation, which has been proven a powerful tool to study adsorption phenomena in nanoporous materials.[21−26] As novelty, we also considered the non-Löwenstein case, which to the best of our knowledge has never been addressed. Although current synthesis techniques do not allow for a tailored placement of the aluminum atoms in zeolites, experimental methods are rapidly improving,[27] which may enable us to achieve significant control over the aluminum distribution in the near future. This way, we aim to exploit further the adsorption properties of zeolites, emphasizing the influence of non-Löwenstein bonds on the adsorption performance of the framework.

The study of the stability of the structures presented in this work is beyond our scope due to the lack of accurate, transferable flexible force[28] and the limitations of DFT to study large systems.[28] Nonetheless, we conducted molecular mechanics simulations to optimize a reference set of structures. The results demonstrate that the adsorption properties do not change significantly before and after minimization. These findings are included in the Supporting Information. We focus here on the identification of patterns in the adsorption properties of non-Löwenstein zeolites, while leaving the investigation of their structural stability aside. This is the first step toward developing a machine learning architecture to comprehend and forecast adsorption properties in non-Löwenstein zeolites.

METHODS

Zeolite Frameworks. Three zeolites have been used to consider a different topology for each pore size: MOR (large pore), MFI (medium pore), and ITW (small pore). MOR-type zeolites have an orthorhombic unit cell with one-dimensional channels along the *c*-axis, which we call main channels or C-channels. The unit cell contains in this case 48 T atoms (Si or Al), which are split in 4 classes of equivalent positions under the action of its space group. Their multiplicities are 16 for T1 and T2 and 8 for T3 and T4. MFI-type zeolites consist of longitudinal and zigzag channels, which are parallel to the crystallographic axes *a* and *b*, respectively. Because these channels are interconnected, the framework has a 3D-channel structure. The unit cell contains 96 T atoms, which can be split in 12 equivalency classes, each one of multiplicity 8. MFI zeolites can be found in two different phases (orthorhombic and monoclinic), and only the orthorhombic lattice was considered. Finally, ITW zeolite has a monoclinic unit cell with 3 nonequivalent T atoms. It possess an extremely fine pore structure, which makes the size of the molecules that can diffuse along the framework very small. The atomic coordinates of all frameworks were taken from the IZA database.[29]

Generation of Aluminum Distributions. The main goal of this work is to study the influence of different aluminum distributions in the adsorption properties of zeolites. In particular, we are interested in the effect of the non-Löwenstein bonds. Therefore, we implemented a series of algorithms to generate zeolite structures stochastically, where the aluminum distributions are sampled from different probability distributions. These algorithms and their details were published as open software under the name of Zeoran and can be found in GitHub (https://github.com/promerma/zeoran). We defined 4 different types of structures. One (chains): frameworks with a given distribution of chains of consecutive Al−O−Al bonds. Two (cluster): frameworks with a cluster of aluminum atoms, i.e., a certain number of aluminum substitutions localized in a small region of the space. Three (maximal entropy): frameworks with a certain number of aluminum atoms spread along the structure, maximizing the average one-to-one distance between them. Four (random): frameworks obtained from a uniform distribution of all possible aluminum distributions. All results presented in this work are based on the analysis of sets of frameworks from the aforementioned types. Type 1 was used to study the effects of a gradual increase in the number of non-Löwenstein bonds. Types 2 and 3 were used as extreme cases, where the number of non-Löwenstein bonds is large and small, respectively. Finally, structures of type 4 were used for comparison purposes.

Findley et al.[20] proposed a different method for the generation of aluminum distributions in Löwenstein zeolites, which is based on a reverse Monte Carlo scheme. However, we believe that the one used in this work might be more appropriate for the goal of our research, for two different reasons. First of all, our method considers the chain distribution, that is, an aluminum distribution not included in the aforementioned paper. This is relevant in our study, as it allows us to accurately obtain structures with a certain number of non-Löwenstein bonds. The second reason is that the reverse Monte Carlo method introduces noise into the generated distributions. This is inconvenient when aiming to compare the extreme cases of very high and very low amounts of non-Löwenstein bonds.

The initial distribution of cations is also stochastic, and it is determined in the equilibration phase of the Monte Carlo simulation. The specific distribution depends on the topology and number and distribution of aluminum atoms. However, in all cases we see that the cations remain close to the oxygen atoms that are bonded to aluminum atoms (i.e., Oa and Oaa) because this is energetically favorable. Besides, cations tend to repel each other according to the Coulombic interaction.

Computational Details. The strength of the interactions between the CO_2 molecules and the zeolites were studied via the heat of adsorption ($-\Delta H$). This property can be calculated using a single adsorbate molecule (the guest molecule) and can be expressed as

$$-\Delta H = \Delta U - RT \quad (1)$$

where ΔU is the difference in internal energy before and after the guest molecule is adsorbed on the framework. To calculate the heat of adsorption, we performed Monte Carlo simulations using the Widom particle insertion method in the canonical ensemble (NVT).[30] This method was also used to calculate the helium void fraction for all the frameworks used in this work, which is needed to obtain the excess adsorption during the simulations. For the validation of our force field, we also calculated adsorption isotherms. These were obtained via Monte Carlo simulations in the grand canonical ensemble (μVT). All simulations were performed with the RASPA software.[31]

https://doi.org/10.1021/acs.chemmater.3c01258
Chem. Mater. 2023, 35, 5222−5231

Simulations were performed at 298 K. The number of equilibration cycles was 5×10^3 in all cases, and the number of the production cycles depends on the simulation experiment. We used 5×10^4 cycles for the void fraction calculations, 7.5×10^4 for the heats of adsorption, and 1.5×10^5 for the adsorption isotherms. For each cycle, the number of MC trial moves is the maximum between the number of molecules in the system and 20. We considered a supercell of $2 \times 2 \times 2$ unit cells for MFI, of $2 \times 2 \times 4$ for MOR, and of $3 \times 2 \times 3$ for ITW to make sure that the dimensions of all systems are at least twice the cutoff distance of the force field in the three Cartesian directions.

We modeled all zeolites and adsorbents as rigid. Although diffusion coefficients are found to be strongly dependent on the flexibility of the framework,[32−34] adsorption simulations done in rigid zeolite frameworks provide results that are in excellent agreement with experimental data.[35−38] Furthermore, because the adsorbate in our case is a small molecule, the distortion of the zeolite in a flexible model would be negligible in most cases. This simplification allowed us to study a wide range of frameworks by reducing the runtime of the simulations some orders of magnitude.

The force field used considers Coulombic potentials for the long-range interactions and Lennard-Jones potentials to account for the van der Waals. Lennard-Jones interactions were truncated at 12 Å and shifted to 0 at the cutoff distance. Given that we considered a rigid framework, interactions between the framework atoms (Si, Al, and O) were not considered. For the van der Waals interactions, we assumed that the zeolite interacts with the adsorbates and the extraframework cations only via the oxygens. This is common way to model the screening effect that the oxygen atoms exert on the silicon and aluminum atoms.[24,38−40] The Coulombic interactions in the system were obtained using the Ewald summation method.[41] The Lennard-Jones parameters and point charges (including those for the dummy atoms) were taken from García-Sánchez et al.,[42] which distinguishes between an oxygen atom binding two silicon atoms (O) and an oxygen atom binding a silicon and an aluminum atom (O_a). Furthermore, the idea of introducing an oxygen pseudoatom was generalized to account for non-Löwenstein bonds in the framework. Namely, we defined another particle (O_{aa}) to model the oxygen atoms binding two aluminum atoms, whose charge was obtained by imposing the charge neutrality condition of the zeolite. A complete description of the interactions and the set of charges used is shown in Table 1. This table shows that the charges between the different oxygen atoms of the zeolite are very similar. Therefore, we do not expect a fictional charge accumulation that would lead to nonphysical results. For the Löwenstein case, the computational framework described here is identical with the one presented in the work of García-Sánchez et al.,[42] which has been validated in a variety of zeolites with different topologies and compositions.

For the CO_2 adsorbates we used the well-validated model of Harris and Yung.[43] This consists of three Lennard-Jones sites in a linear geometry with point charges centered at each atom. The distance between the carbon and oxygen atoms was taken equal to 1.149 Å. Finally, the sodium cations were represented as single point charges and were modeled as mobile, meaning that their position was the result of their interactions with the zeolite, the adsorbents, and the other cations.

Given the lack of experimental data available for non-Löwenstein zeolites, a direct validation of the force field is not possible in that case. However, the use of this force field is motivated by the fact that it reproduces the expected adsorption properties. Indeed, Figure 1a shows that different Löwenstein and non-Löwenstein aluminum distributions in MFI lead to the same loading at saturation pressure. This is what we would expect because the MFI zeolite does not contain inaccessible sites for the CO_2 molecules, which implies that at very high pressures the amount of carbon dioxide adsorbed is dictated solely by the void fraction of the zeolite. Although the void fraction is sensitive to the number of aluminum substitutions (as the cations leave less space for the adsorbents), it is not dependent on the exact positions of these atoms. For MOR (Figure 1b) we did not reach saturation, as at room temperature this requires going to very high pressures, which is expensive and unrealistic. However, at this range, the isotherms are also expected to converge, for the same reason we mentioned above. Notice that in MOR the loading at saturation pressure will be higher than for MFI because it has a larger accessible volume. Besides, Figure 1 shows a continuous deviation from the Löwenstein case when longer chains are considered for both topologies. This shows that introducing non-Löwenstein bonds into the system does not break the structural properties of the material and that the force field used can accurately capture the effects of these linkages.

Table 1. Point Charges and Force Field Parameters for CO_2 Adsorption Simulations in Non-Löwenstein Zeolites

atom(s)	LJ parameter ϵ/k_B [K]	LJ parameter σ [Å]	charge [e]
Si			0.78598
Al			0.48598
O			−0.39299
O_a			−0.41384
O_{aa}			−0.43469
Na	124.400	2.160	0.38340
He	10.900	2.640	0
O_{CO_2}	85.671	3.017	−0.32560
C_{CO_2}	29.933	2.745	0.65120
He−Na	36.823	2.400	
O_{CO_2}−C_{CO_2}	50.640	2.880	
O_{CO_2}−O	78.980	3.237	
O_{CO_2}−O_a	78.980	3.237	
O_{CO_2}−O_{aa}	78.980	3.237	
C_{CO_2}−O	37.595	3.511	
C_{CO_2}−O_a	37.595	3.511	
C_{CO_2}−O_{aa}	37.595	3.511	
O_{CO_2}−Na	200.831	2.758	
C_{CO_2}−Na	362.292	3.320	
O−Na	23.000	3.400	
O_a−Na	23.000	3.400	
O_{aa}−Na	23.000	3.400	

RESULTS AND DISCUSSION

For each topology we considered different Si/Al ratios. In fact, part of our study focuses not only on the Al distribution but also on the effect of the number of substitutions. As we detailed in the Introduction, we analyzed the effect of (a) the Si/Al ratio and (b) the aluminum distribution on the adsorption properties of carbon dioxide in three zeolites. The adsorption was quantified via the heat of adsorption ($-\Delta H$), which is an indicator of the strength of the interaction between an adsorbate and a solid adsorbent. For each particular zeolite we started with just one Al substitution, and then we increased it sequentially. For clarity, we mention explicitly the number of Al substitutions in the text and figures, instead of the Si/Al ratios. The maximum number of substitutions is different for each zeolite: 32 for MFI, 28 for MOR, and 10 for ITW, which corresponds to Si/Al ratios of 2, 1, and 1.4, respectively.

Effect of the Al Distribution in MFI. The adsorption properties of the MFI zeolite are determined by its wide 3D-channel structure. Figure 2 shows that there are no preferred adsorption sites for the CO_2 molecules in the all-silica framework of this topology. In the aluminosilicate structures, the sodium cations break the channel homogeneity by creating adsorption sites, as they interact with the carbon dioxide molecules, favoring adsorption. Then because the cations are

https://doi.org/10.1021/acs.chemmater.3c01258
Chem. Mater. 2023, 35, 5222−5231

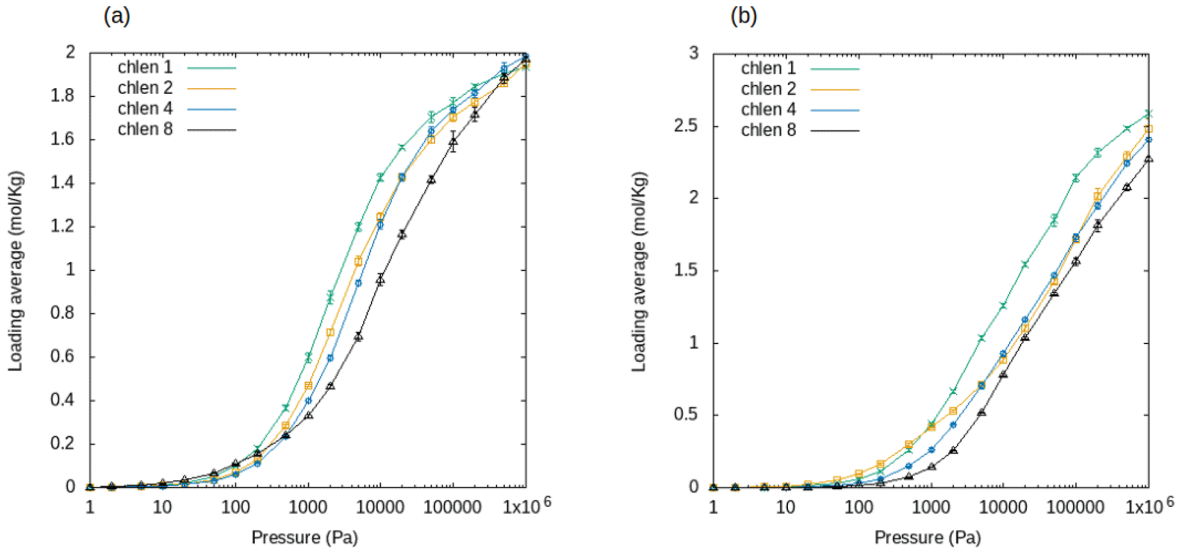

Figure 1. CO_2 adsorption isotherms for (a) MFI and (b) MOR. In both cases, all the structures contain 8 Al substitutions, which are distributed in chains of equal length (chlen).

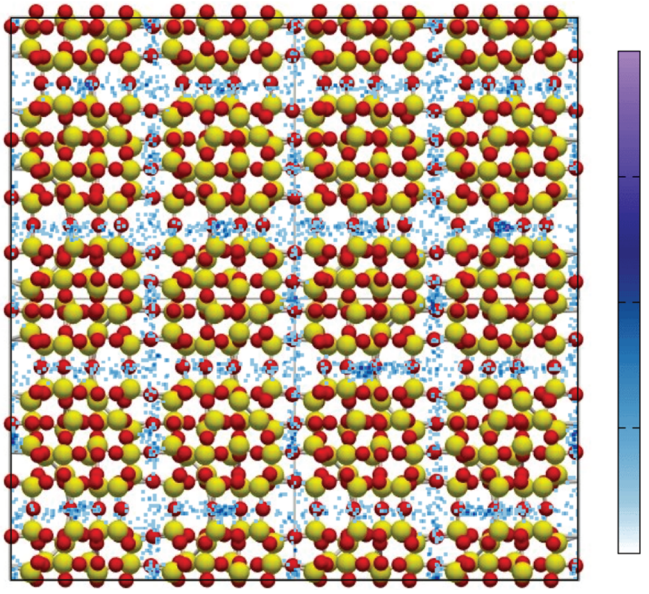

Figure 2. Adsorption sites of the carbon dioxide molecules in the all-silica MFI zeolite viewed from the plane perpendicular to the *c*-axis. Atoms in yellow correspond to Si and in red to O.

adsorbed near the aluminum substitutions, one would expect the adsorption behavior of this topology to be highly dependent on the aluminum distribution.

Figure 1a shows that for mid-high pressures the structures with longer chains lead to a slightly lower loading average. This is attributed to the van der Waals repulsion between different CO_2 molecules. The longer aluminum chains create fewer but more attractive adsorption sites because the cations are more clusterized in the structure. However, the van der Waals interactions between the CO_2 molecules prevent many of them from being adsorbed. On the contrary, when the Al atoms are spread along the framework (shorter chain distributions), there are many low-interacting adsorption sites, which lead to a higher loading average.

The values of the heat of adsorption in the MFI zeolite are shown in Figure 3. The heat of adsorption is highly dependent on the total number of aluminum substitutions but barely affected by the lengths of the aluminum chains. We see that the heat of adsorption remains constant when increasing the length of the chains for all the amounts of Al atoms. This result differs from what we found in the study of the adsorption isotherms (where the chain distribution affected the loading) and can be explained by the principles of the particle insertion method. In particular, because the heat of adsorption is measured from a single adsorbate molecule, the interaction between multiple CO_2 molecules does not play any role here. Furthermore, the wide-channel topology of the framework (compared to the size of the CO_2 molecule) implies that the cations will be sufficiently distant from each other, as a result of to the Coulombic repulsion. Consequently, the single CO_2 molecule will be adsorbed near a single cation, regardless of the aluminum distribution.

To corroborate that the amount of non-Löwenstein bonds does not affect the heat of adsorption, we compared two extreme sets of structures: the cluster and maximal entropy, described in the Methods section. As shown in Figure 3b, the values of the heat of adsorption for both sets are compatible within the error bars. However, the standard deviation of the cluster set is in all cases much higher than for the other sets. This follows from the fact that having more aluminum atoms together drastically increases the amount of interactions located in small regions of the space, which leads to higher errors in the simulations. Finally, the averaged values over random structures show a damped increase of the heat of adsorption as a function of the number of Al atoms when this is smaller than 4, followed by a linear regime. The damped-increase regime is due to the fact that the addition of the first Al substitution results in the most drastic change of the molecular environment of the framework, as compared to adding one more Al atom when the Si/Al ratio is finite. For smaller Si/Al ratios, the increase in the heat of adsorption when a new Al atom is added stabilizes, leading to the linear regime. Overall, these results show that in MFI the heat of adsorption is more dependent on the number of Al atoms rather than on its specific distribution.

Effect of the Al Distribution in MOR. To evaluate if the behavior obtained for the MFI zeolite can be generalized to

https://doi.org/10.1021/acs.chemmater.3c01258
Chem. Mater. 2023, 35, 5222−5231

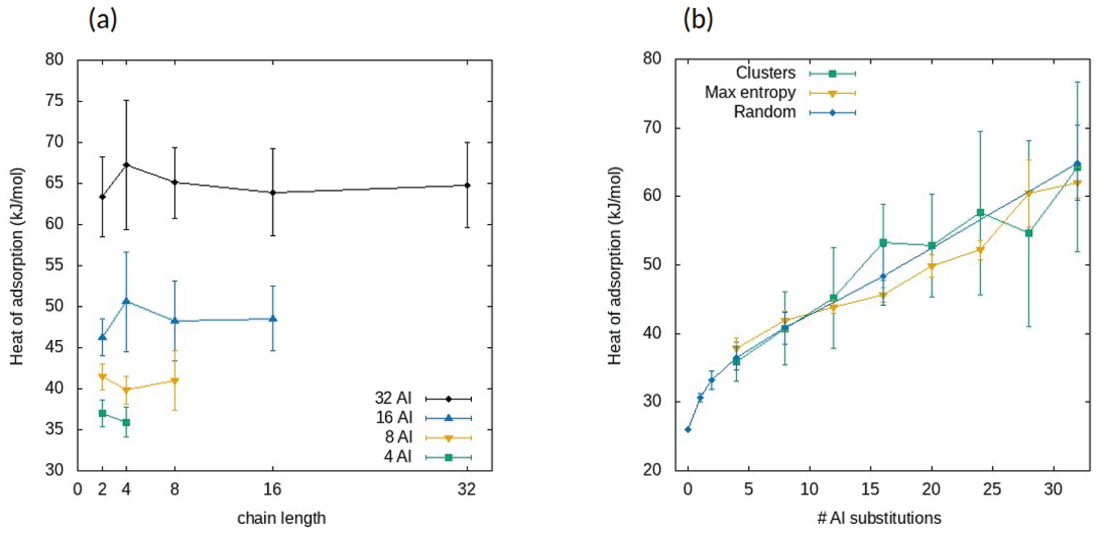

Figure 3. (a) Heat of adsorption of carbon dioxide in chain structures as a function of their chain length, for multiple numbers of aluminum substitutions in MFI. All chains of a given structure are of the same length. Each point corresponds to average results over 20 structures, and the error bars are the corresponding standard deviations. (b) Heat of adsorption as a function of the number of aluminum atoms in the system for multiple sets of MFI structures. For the cluster and maximal entropy sets, each point corresponds to the average value over 20 structures. The points corresponding to the random set corresponds to the average over 50 random structures.

other zeolites, we studied topologies with large and small pore as well. We selected MOR as representative of large pore zeolites. Figure 4 shows the average occupation profile of the carbon dioxide molecules inside the framework, viewed from the [0,0,1] direction. Given the 1D-channel structure of the MOR zeolite, it is sufficient to analyze only this view. We notice that in the all-silica framework, there are two adsorption sites for CO_2 molecules: in the main channels along the *c* direction and inside the 4-atom rings, which are the so-called side pockets. The fact that the beads that form the side pockets correspond to a single atom favors the interaction between the framework oxygen and the carbon atom of the adsorbate. Hence, in the side pockets the CO_2 is adsorbed closer to the zeolite. However, when Al atoms are included in the framework, the cations tend to fill the side pockets, leaving no space for the carbon dioxide to be adsorbed there. Given the small size of the sodium atoms, the side pockets are very energetically favorable adsorption sites for these atoms. Thus, in the presence of Al substitutions, the molecules of carbon dioxide will be adsorbed only in the main channels.

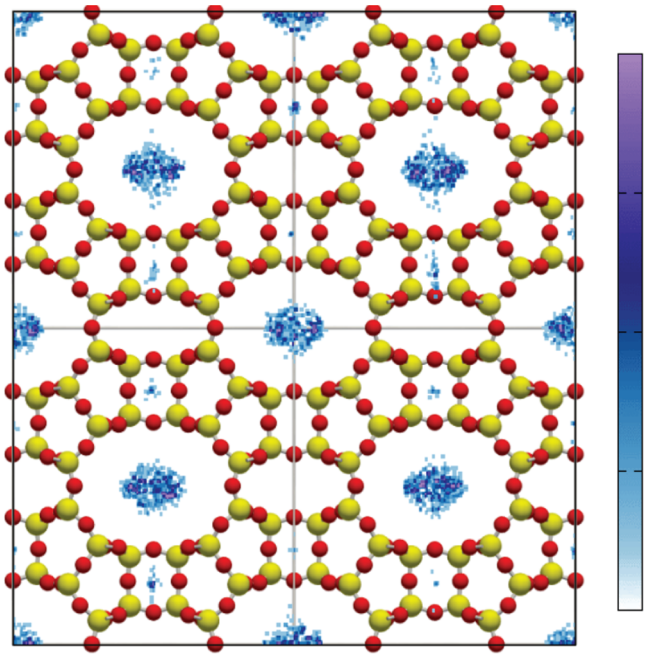

Figure 4. Adsorption sites of the carbon dioxide molecules in the all-silica MOR zeolite viewed from the plane perpendicular to the *c*-axis. Atoms in yellow correspond to Si and in red to O. The beads corresponding to all the atoms that do not belong to a side pocket (4-atom ring) have multiplicity 2, meaning that they represent two atoms with different *z* coordinates, but the same (*x*, *y*). The multiplicity of the atoms of the side pockets is one.

Figure 5a shows the influence of the aluminum substitutions in the different T sites on the adsorption. The heat of adsorption is considerably smaller when we have aluminum substitutions in the T3 position. This behavior was reported by Zhakisheva et al. in the adsorption of water,[39] where all frameworks analyzed obeyed the Löwenstein rule. This lower value of the heat of adsorption can be explained by looking at the sodium cations. Figure 5b shows that when aluminum atoms are placed in all the T3 positions, only about 18% of the sodium atoms are contained in the main channel. This value is considerably smaller than in the other cases, where it is roughly the 50%. Indeed, the atoms in T3 are the only ones that do not belong to the main channel. In this case, the number of cations in the main channel is the lowest, as Coulombic interactions attract the sodium cations to the aluminum atoms. Given the number of aluminum substitutions in the framework, the CO_2 molecules will be adsorbed in the main channels rather than in the side pockets with a probability higher than 0.99. Hence, the higher concentration of sodium cations in the main channels in the cases of T1, T2, and T4 results in more and stronger interactions between the sodium atoms and the adsorbate, which leads to a higher heat of adsorption. We then conclude that placing the Al atoms in T3 decreases the heat of adsorption, as compared to placing them in other positions. In

https://doi.org/10.1021/acs.chemmater.3c01258
Chem. Mater. 2023, 35, 5222−5231

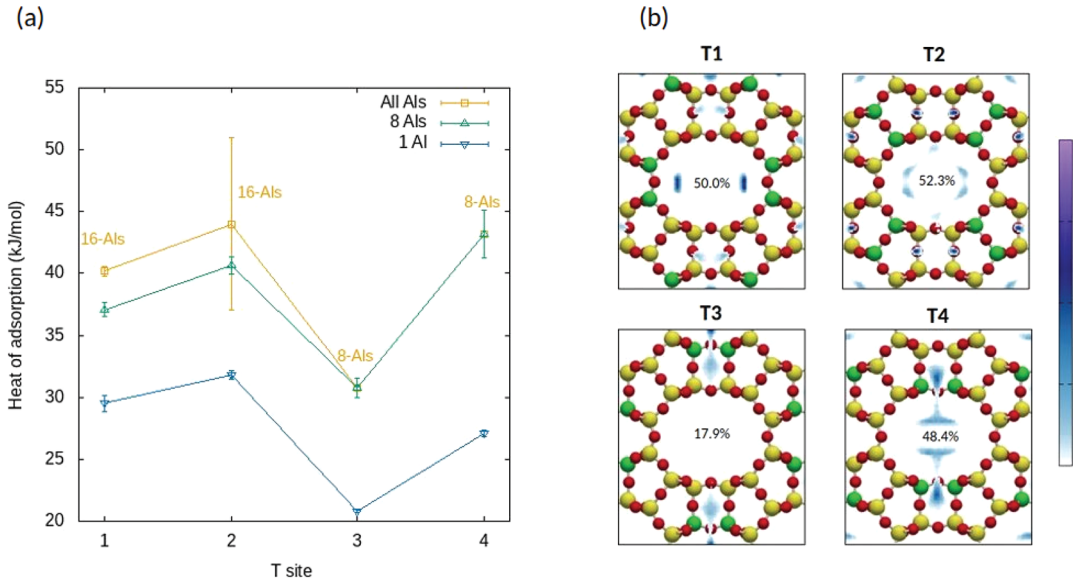

Figure 5. (a) Heat of adsorption as a function of the T position in MOR for different number of aluminum substitutions. (b) Adsorption sites of the sodium cations in the 4 MOR frameworks where all equivalent positions contain aluminum atoms. The percentages correspond to the amount of sodium cations confined in the main channel.

fact, Figure 6 shows that when a higher concentration of the Al atoms are placed in T3, the heat of adsorption becomes lower.

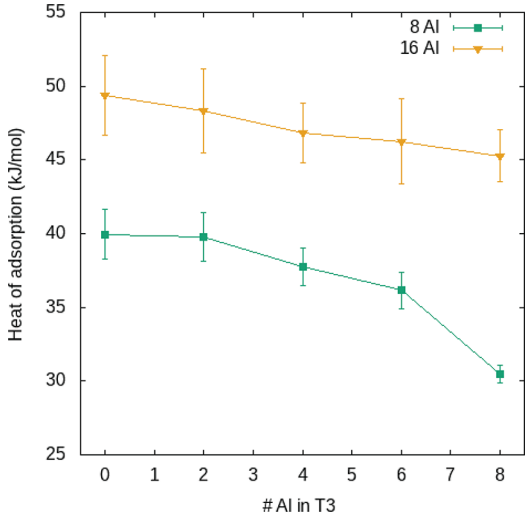

Figure 6. Heat of adsorption as a function of the number of Al atoms in the T3 position for random MOR frameworks with 8 and 16 Al substitutions. Each point corresponds to the average value over 20 structures and the error bars to the standard deviations.

To study the influence of the amount of non-Löwenstein bonds in the resulting heat of adsorption, we used the cluster and maximal entropy structures described in the Methods section. For different numbers of aluminum substitutions, we randomly created 20 structures of each type and performed simulations to calculate the heat of adsorption for each case. The results are depicted in Figure 7 and show a consistent trend where the maximal entropy structures lead to a higher heat of adsorption. This finding was initially unexpected because a higher spatial concentration of aluminum atoms results in a higher concentration of cations in a nearby region, which should enhance the adsorption of carbon dioxide due to the higher amount of interactions. However, by analyzing individually multiple structures of both types, we found that rather than the concentration of sodium cations, what influences the heat of adsorption is their distribution inside the main channel.

Figure 7a shows the distribution of the sodium cations in two different structures with 9 aluminum substitutions corresponding to the maximal entropy set (yellow diamond) and clusters set (green diamond). In the cluster structure, the cations inside the main channel are confined in the vicinity of the cluster of aluminum atoms, located in the bottom right corner of the figure. Instead, as in the maximal entropy structure, the aluminum substitutions are spread over the zeolite; the cations inside the main channel occupy a larger volume of the channel. As argued before, in both cases the carbon dioxide molecules will be adsorbed inside the main channel. Thus, in the maximal entropy structure this molecule will be surrounded by a greater number of cations, which will lead to a higher number of interactions and, hence, to a higher value of the heat of adsorption. These results are in agreement with the ones reported for the study of the different T positions. In particular, they all suggest that there are two main factors influencing the adsorbing properties of CO_2 in MOR: the number of cations inside the main channel and their distribution. We expect a higher value of the heat of adsorption when there is a large number of sodium cations inside the main channel homogeneously distributed because this favors the interactions between the adsorbate and the framework via the extraframework cations. To validate this hypothesis, we considered two structures with a cation distribution that fulfills these conditions. Namely, we defined two structures with all the aluminum substitutions belonging to the T positions T1, T2, and T4, which are the ones belonging to the main channel of the zeolite. Moreover, we impose these substitutions to be contained in one of the two main channels of the unit cell: the one in the center. Finally, we consider the substitutions to be spread along the channel surface. By doing this, we aim to restrict the majority of the cations to this channel as homogeneously distributed as possible. These frameworks are shown in Figure 7c.

https://doi.org/10.1021/acs.chemmater.3c01258
Chem. Mater. 2023, 35, 5222−5231

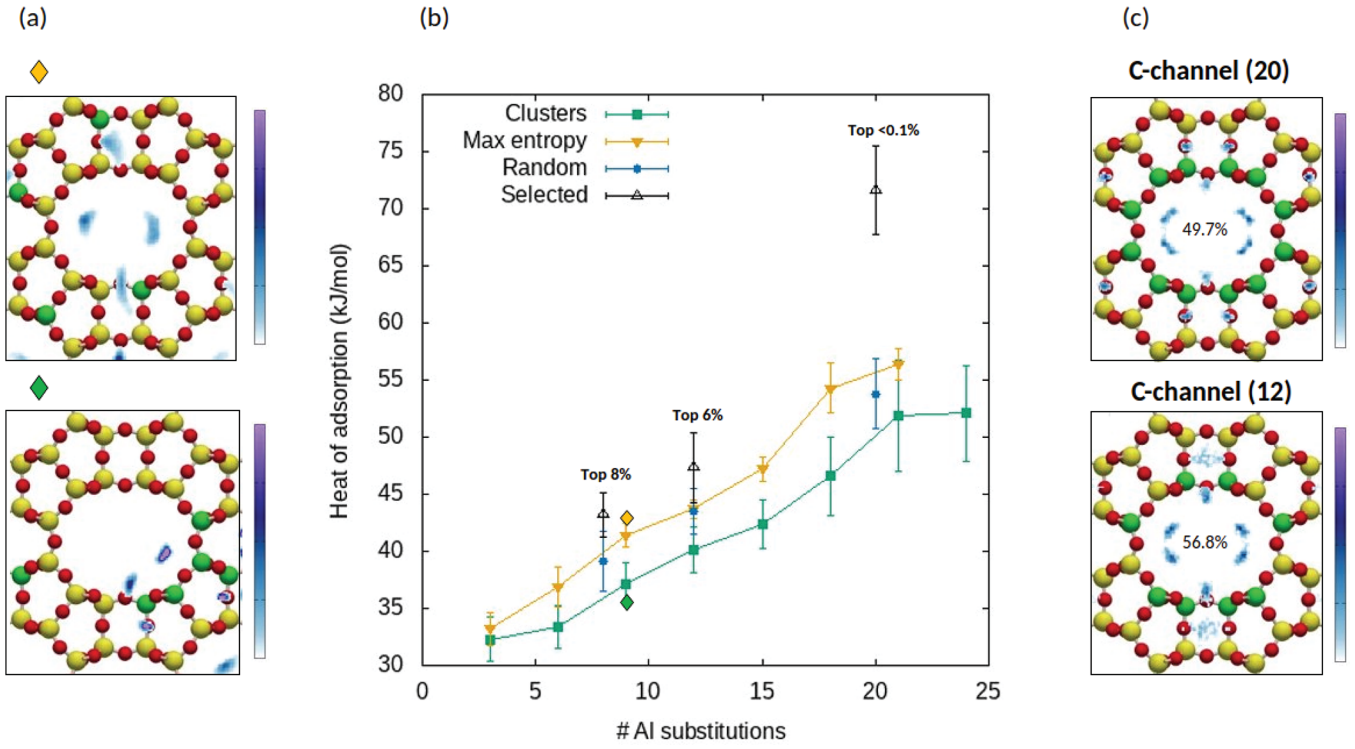

Figure 7. (a) Sodium distribution in two selected MOR structures with 9 aluminum substitutions. Notice that not all the aluminum substitutions can be seen in the image because some of them are in T sites with a deeper z coordinate. (b) Heat of adsorption as a function of the number of aluminum atoms in the framework for multiple sets of MOR structures. Filled points show averaged values over 20 structures for the clusters and maximal entropy sets and over 200 structures for the random set, while error bars show the standard deviations. Open points represent values of single structures and the corresponding error bars are the simulation errors. The selected set contains three structures: the framework with aluminum sites in T4 (8 Al) and 2 frameworks with an Al distribution in the T atoms of the main channel found in the middle of the unit cell (12 and 20 Al). (c) Sodium distribution in the selected MOR frameworks with 12 and 20 Al atoms viewed from the [0,0,1] direction.

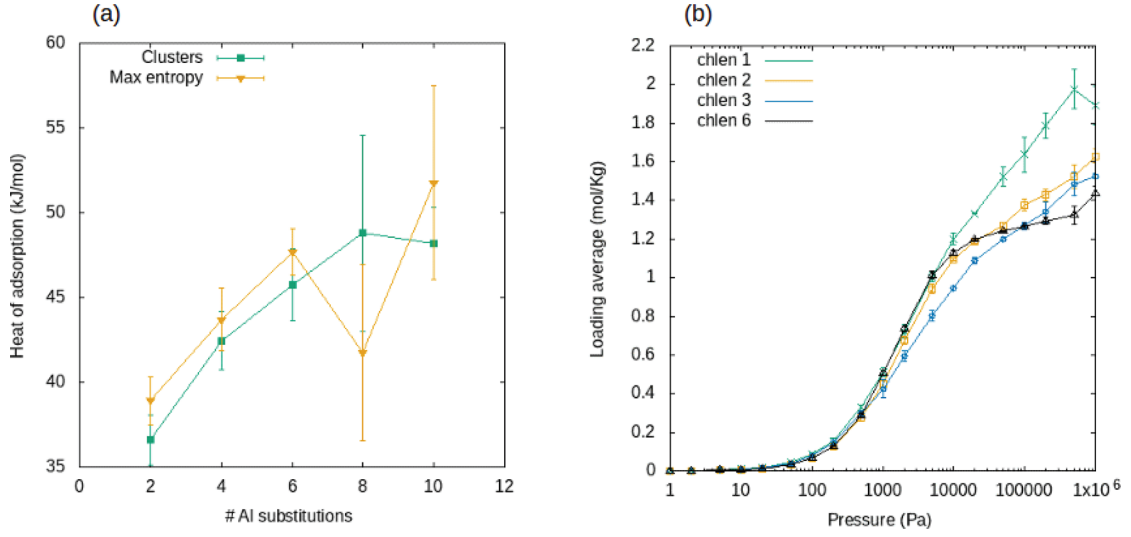

Figure 8. (a) Heat of adsorption as a function of the number of aluminum atoms in the framework for clusters and maximal entropy ITW structures. Every point corresponds to the average of 20 different distributions and the error bars show the standard deviations. (b) CO_2 adsorption isotherms for ITW structures with chain distributions. All structures contain 6 Al substitutions, grouped in different chains of the same length in each structure.

To assess the adsorption properties of these frameworks, we compared their heat of adsorption with this magnitude for random structures with the same number of aluminum atoms. The averaged results for the random structures with 8, 12, and 20 substitutions are shown in Figure 7b, and in all cases they fall within the values limited by the cluster and maximal entropy structures. This is what we would expect because the cluster and maximal entropy structures correspond to extreme cases in the distribution of all possible structures. We found that the results for the random structures are closer to the maximal entropy than to the clusters because random

https://doi.org/10.1021/acs.chemmater.3c01258
Chem. Mater. 2023, 35, 5222−5231

structures are statistically more likely to maximize the entropy of the system rather than to create clusters of aluminum atoms.

The resulting heat of adsorption of the candidate structures are also shown in Figure 7b. There, we can see that these structures lead to a higher heat of adsorption compared to the random, cluster, and maximal entropy structures. Figure 7c shows that in all cases we achieve a relatively uniform cation distribution in the peripheral region of the main channel. Furthermore, the proportion of cations inside the main channels is relatively high, and in contrast to the results shown in Figure 5b, now all the sodium atoms in the main channel are restricted to the one in the middle of the unit cell. Hence, we considerably increased the filling of cations in a given channel.

Effect of the Al Distribution in ITW. In order to account for a topology of small-pore zeolite, we conducted a similar study in the ITW framework. Molecular dynamics simulations showed that the small openings of the cages in ITW restrict the diffusion of CO_2 molecules along the structure, confining them to their initial cage. The heat of adsorption was only examined for a narrow range of the number of Al atoms due to the small pore size distribution, which limits the number of molecules that can be adsorbed in the framework. When too many Al substitutions are considered, the cation−cation and cation−adsorbate interactions increase, resulting in higher values of the heat of adsorption per number of Al atoms compared to MOR and MFI. These interactions are also responsible for instabilities, resulting in high simulations errors. Figure 8a shows that for 8 Al atoms the error bars are already too big to obtain significant results. For smaller numbers of Al atoms, we see that the maximal entropy structures perform slightly better. When the Al atoms are distributed in the cluster fashion, the cations occupy the entire available space of the cages where they are located, leaving no space for the carbon dioxide molecule. Consequently, this is adsorbed next to the cloud instead of inside it, which decreases the number of interactions and leads to a slightly smaller value of the heat of adsorption.

The effect of the small pore can also be inferred from the adsorption isotherms presented in Figure 8b, which show that the saturation occurs at a lower pressure when compared to MFI. Similarly, the loading at saturation is also lower in this case because there is less accessible volume in this topology. Furthermore, this figure shows that saturation pressure and loading at this pressure decrease for the longer Al chains distributions. In MFI, there were differences in the loadings in the mid-pressure range, but not at saturation pressure, where all the isotherms converged. This is due to the channel topology of the MFI zeolite, which allows a higher compressibility of the adsorbed molecules. Instead, in ITW the strong interactions of different number of cations in the same cage change the total number of molecules of carbon dioxide that can be adsorbed, leading to different loadings at the high pressure range. However, by increasing pressure even further, at some point all the isotherms would converge, as the accessible volume is equal in all the frameworks. Nonetheless, it is not relevant to study higher pressures, as for those carbon dioxide would be in the liquid phase.

CONCLUSIONS

We proposed a new set of charges for zeolites that generalize a transferable force field which accounts for non-Löwenstein linkages to study carbon dioxide adsorption in zeolites. The resulting force field was used to characterize the heat of adsorption of the MFI and MOR topologies as a function of the aluminum distributions. We found that in MFI the heat of adsorption depends mainly on the number of Al atoms. In fact, due to its wide 3D-channel structure, the CO_2 molecule is adsorbed close to a single cation, meaning that the exact position of the other cations (and hence the Al atoms) are not relevant to the heat of adsorption. In particular, the amount of non-Löwenstein bonds does not significantly affect this magnitude.

For MOR zeolites, the study of the Al substitutions in the different T sites revealed significant differences in the heat of adsorption. The sites that form the C-channel lead to a higher heat of adsorption when an Al atom is placed there, as it confines the cation closer to the CO_2 molecule, which is also adsorbed into the channel. In this case, the influence of the number of non-Löwenstein linkages was notable, as in general when this is higher the Al atoms are more clusterized. This leads to a less homogeneous distribution of the cations in the channel, which reduces the interactions between the framework and the adsorbate. This idea was used to create frameworks with Al distributions that would make the cation distributions to be as uniform as possible inside the C-channel. Such structures contained consecutive Al−O−Al linkages, but they were not clusterized in a small region. We found that these frameworks exhibit a very high heat of adsorption as compared to other structures with the same number of Al atoms. This claims for the potential impact of the Al−O−Al bonds in the MOR zeolite.

Finally, the small pore-size distribution of the ITW topology did not allow us to carry out a complete study. In this framework, the cations and the adsorbate were confined in small cages, leading to strong interactions and high simulation errors. Nevertheless, for the higher Si/Al ratios tested, a small preference for the maximal entropy structures was observed. Besides, we noticed that the loading pressure was smaller than for MFI and MOR, as the accessible volume is also smaller.

ASSOCIATED CONTENT

Supporting Information

The Supporting Information is available free of charge at https://pubs.acs.org/doi/10.1021/acs.chemmater.3c01258.

Energy minimization of a selected set of frameworks (PDF)

AUTHOR INFORMATION

Corresponding Authors

Juan José Gutiérrez-Sevillano − *Department of Physical, Chemical and Natural Systems, University Pablo de Olavide, 41013 Seville, Spain;* orcid.org/0000-0001-8224-839X; Email: jjgutierrez@upo.es

Sofia Calero − *Department of Applied Physics and Science Education, Eindhoven University of Technology, 5612AZ Eindhoven, Netherlands;* orcid.org/0000-0001-9535-057X; Email: s.calero@tue.nl

Author

Pablo Romero-Marimon − *Department of Applied Physics and Science Education, Eindhoven University of Technology, 5612AZ Eindhoven, Netherlands;* orcid.org/0000-0001-9164-6541

Complete contact information is available at: https://pubs.acs.org/10.1021/acs.chemmater.3c01258

https://doi.org/10.1021/acs.chemmater.3c01258
Chem. Mater. 2023, 35, 5222−5231

Notes

The authors declare no competing financial interest.

■ ACKNOWLEDGMENTS

This study was funded by the Spanish Ministerio de Ciencia e Innovacion (IJC2018-038162-I). We thank C3UPO for the HPC support.

■ REFERENCES

(1) Sneddon, G.; Greenaway, A.; Yiu, H. The potential applications of nanoporous materials for the adsorption, separation, and catalytic conversion of carbon dioxide. *Adv. Energy. Mater.* **2014**, *4*, 1301873.
(2) González-Olmos, R.; Gutiérrez-Ortega, A.; Sempere, J.; Nomen, R. Zeolite versus carbon adsorbents in carbon capture: A comparison from an operational and life cycle perspective. *J. of CO_2 utilization* **2022**, *55*, 101791.
(3) Gargiulo, N.; Pepe, F.; Caputo, D. CO_2 adsorption by functionalized nanoporous materials: a review. *J. of Nanoscience and Nanotechnology* **2014**, *14*, 1811−1822.
(4) Khaleque, A.; Alam, M.; Hoque, M.; Mondal, S.; et al. Zeolite synthesis from low-cost materials and environmental applications: A review. *Environmental Advances* **2020**, *2*, 100019.
(5) Cruciani, G. Zeolites upon heating: Factors governing their thermal stability and structural changes. *J. Phys. Chem. Solids* **2006**, *67*, 1973−1994.
(6) Derbe, T.; Temesgen, S.; Bitew, M. A short review on synthesis, characterization, and applications of zeolites. *Adv. Mater. Sci. Eng.* **2021**, *2021*, 6637898.
(7) Gutiérrez-Sevillano, J. J.; Caro-Pérez, A.; Dubbeldam, D.; Calero, S. Molecular simulation investigation into the performance of Cu-BTC metal-organic frameworks for carbon dioxide-methane separations. *J. Phys. Chem. Chem. Phys.* **2011**, *13*, 20453−20460.
(8) Gutiérrez-Sevillano, J. J.; Vicent-Luna, J. M.; Dubbeldam, D.; Calero, S. Molecular mechanisms for adsorption in Cu-BTC metal organic framework. *J. Phys. Chem. C* **2013**, *117*, 11357−11366.
(9) Vikrant, K.; Kumar, V.; Kim, K.; Kukkar, D. Metal-organic frameworks (MOFs): potential and challenges for capture and abatement of ammonia. *J. Mater. Chem. A* **2017**, *5*, 22877−22896.
(10) Bonenfant, D.; Kharoune, M.; Niquette, P.; Mimeault, M.; Hausler, R. Advances in principal factors influencing carbon dioxide adsorption on zeolites. *Sci. Technol. Adv. Mater.* **2008**, *9*, 013007.
(11) Yang, C.; Janda, A.; Bell, A.; Lin, L. Atomistic investigations of the effects of Si/Al ratio and Al distribution on the adsorption selectivity of n-Alkanes in Bronsted-Acid zeolites. *J. Phys. Chem. C* **2018**, *122*, 9397−9410.
(12) Moradi, H.; Azizpour, H.; Bahmanyar, H.; Rezamandi, N.; Zahedi, P. Effect of Si/Al ratio in the faujasite structure on adsorption of methane and nitrogen: a molecular dynamics study. *Chem. Eng. Technol.* **2021**, *44*, 1221−1226.
(13) Choi, H.; Jo, D.; Hong, S. Effect of framework Si/Al ratio on the adsorption mechanism of CO_2 on small pore zeolites: II. Merlinoite. *Chem. Eng. J.* **2022**, *446*, 137100.
(14) Loewenstein, W. The distribution of aluminum in the tetrahedra of silicates and aluminates. *Am. Mineral.* **1954**, *39*, 92−96.
(15) Fletcher, R.; Ling, S.; Slater, B. Violations of Loewenstein's rule in zeolites. *Chem. Sci.* **2017**, *8*, 7483−7491.
(16) Pavón, E.; Osuna, F.; Alba, M.; Delevoye, L. Direct evidence of Lowenstein's rule violation in swelling high-charge micas. *Chem. Commun.* **2014**, *50*, 6984−6987.
(17) Heard, C.; Grajciar, L.; Nachtigall, P. The effect of water on the validity of Löwenstein's rule. *Chem. Sci.* **2019**, *10*, 5705−5711.
(18) Afeworki, M.; Dorset, D.; Kennedy, G.; Strohmaier, K. Synthesis and structure of ECR-40: an ordered SAPO having the MEI framework. *Stud. Surf. Sci. Catal.* **2004**, *154*, 1274−1281.
(19) Bell, R.; Jackson, R.; Catlow, C. Löwenstein's rule in zeolite A: a computational study. *Zeolites* **1992**, *12*, 870−871.
(20) Findley, J. M.; Ravikovitch, P. I.; Sholl, D. S. The effect of aluminum short-range ordering on carbon dioxide adsorption in zeolites. *J. Phys. Chem. C* **2018**, *122*, 12332−12340.
(21) Fuchs, A.; Cheetham, A. Adsorption of guest molecules in zeolitic materials: computational aspects. *J. Phys. Chem. B* **2001**, *105*, 7375−7383.
(22) García-Pérez, E.; Parra, J.; Ania, C.; Dubbeldam, D.; Vlugt, T.; Castillo, J.; Merkling, P.; Calero, S. Unraveling the argon adsorption processes in MFI-type zeolite. *J. Phys. Chem. C* **2008**, *112*, 9976−9979.
(23) Matito-Martos, I.; Martin-Calvo, A.; Gutiérrez-Sevillano, J. J.; Haranczyk, M.; Doblare, M.; Parra, J.; Ania, C.; Calero, S. Zeolite screening for the separation of gas mixtures containing SO2, CO_2 and CO. *J. Phys. Chem. Chem. Phys.* **2014**, *16*, 19884.
(24) Jaraíz-Arroyo, I.; Martin-Calvo, A.; Gutiérrez-Sevillano, J. J.; Barranco, C.; Diaz-Diaz, N.; Calero, S. OCEAN: An algorithm to predict the separation of biogas Using zeolites. *Ind. Eng. Chem. Res.* **2020**, *59*, 7212−7223.
(25) Jajko, G.; Kozyra, P.; Makowski, W.; Gutiérrez-Sevillano, J. J.; Calero, S. Carbon dioxide capture enhanced by pre-adsorption of water and methanol in UiO-66. *Chem.—Eur. J.* **2021**, *27*, 14653−14659.
(26) Martin-Calvo, A.; Gutiérrez-Sevillano, J. J.; Matito-Martos, I.; Vlugt, T. J. H.; Calero, S. Identifying zeolite topologies for storage and release of hydrogen. *J. Phys. Chem. C* **2018**, *122*, 12485−12493.
(27) Velty, A.; Corma, A. Advanced zeolite and ordered mesoporous silica-based catalysts for the conversion of CO_2 to chemicals and fuel. *Chem. Soc. Rev.* **2023**, *52*, 1773−1946.
(28) Dubbeldam, D.; Walton, K.; Vlugt, T.; Calero, S. Design, parameterization, and implementation of atomic force fields for adsorption in nanoporous materials. *Adv. Theory Simul.* **2019**, *2*, 1900135.
(29) Baerlocher, C.; Meier, W.; Olson, D. *Atlas of Zeolite Framework Types*, 5th ed.; Elsevier: 2001.
(30) Widom, B. Some topics in the theory of fluids. *J. Chem. Phys.* **1963**, *39*, 2808−2812.
(31) Dubbeldam, D.; Calero, S.; Ellis, D.; Snurr, R. RASPA: Molecular simulation software for adsorption and diffusion in flexible nanoporous materials. *Mol. Simul.* **2016**, *42*, 81−101.
(32) van den Berg, A.; Bromley, S.; Ramsahye, N.; Maschmeyer, T. Diffusion of molecular hydrogen through porous materials: the importance of framework flexibility. *J. Phys. Chem. B* **2004**, *108*, 5088−5094.
(33) Kopelevich, D.; Chang, H. Diffusion of inert gases in silica sodalite: Importance of lattice flexibility. *J. Chem. Phys.* **2001**, *115*, 9519−9527.
(34) Demontis, P.; Suffritti, G. Molecular dynamics investigation of the diffusion of methane in a cubic symmetry zeolite of type ZK4. *J. Chem. Phys. Lett.* **1994**, *223*, 355−362.
(35) García-Sánchez, A.; Dubbeldam, D.; Calero, S. Modeling adsorption and self-diffusion of methane in LTA zeolites: the influence of framework flexibility. *J. Phys. Chem. C* **2010**, *114*, 15068−15074.
(36) Dubbeldam, D.; Calero, S.; Vlugt, T.; Krishna, R.; Maesen, T.; Beerdsen, E.; Smit, B. Force field parametrization through fitting on inflection points in isotherms. *Phys. Rev. Lett.* **2004**, *93*, 088302.
(37) García-Sánchez, A.; García-Pérez, E.; Dubbeldam, D.; Krishna, R.; Calero, S. A simulation study of alkanes in linde type A zeolites. *S. Adsorpt. Sci. Technol.* **2007**, *25*, 417−427.
(38) Martin-Calvo, A.; Gutiérrez-Sevillano, J. J.; Parra, J. B.; Ania, C. O.; Calero, S. Transferable force fields for adsorption of small gases in zeolites. *Phys. Chem. Chem. Phys.* **2015**, *17*, 24048.
(39) Zhakisheva, B.; Gutiéerez-Sevillano, J.; Calero, S. Ammonia and water in zeolites: Effect of aluminum distribution on the heat of adsorption. *Sep. Purif. Technol.* **2023**, *306*, 122564.
(40) Gutiérrez-Sevillano, J. J.; Calero, S.; Hamad, S.; Grau-Crespo, R.; Rey, F.; Valencia, S.; Palomino, M.; Balestra, S.; Ruiz-Salvador, A. R. Critical Role of Dynamic Flexibility in Ge-Containing Zeolites: Impact on Diffusion. *Chem.—Eur. J.* **2016**, *22*, 10036−10043.

https://doi.org/10.1021/acs.chemmater.3c01258
Chem. Mater. 2023, 35, 5222−5231

(41) Frenkel, D.; Smit, B. *Understanding Molecular Simulations: From Algorithms to Applications*, 2nd ed.; Academic Press: San Diego, CA, 2002.
(42) García-Sánchez, A.; Parra, J.; Dubbeldam, D.; Calero, S.; et al. Transferable force field for carbon dioxide adsorption in zeolites. *J. Phys. Chem. C* **2009**, *113*, 8814−8820.
(43) Harris, J. G.; Yung, K. H. Carbon dioxide's liquid-vapor coexistence curve and critical properties as predicted by a simple molecular model. *J. Phys. Chem.* **1995**, *99*, 12021−12024.

https://doi.org/10.1021/acs.chemmater.3c01258
Chem. Mater. 2023, 35, 5222−5231